BULLETIN OF THE EARTHQUAKE
RESEARCH INSTITUTE
Vol. 44 (1966), pp. 1419-1434

67. *Mechanism of the Hindu Kush Earthquake of Jan. 28, 1964, Derived from S Wave Data: The Use of pP-Phase for the Focal Mechanism Determination.**

By Abolghassem HEDAYATI,**

International Institute of Seismology and Earthquake Engineering
and
Tomowo HIRASAWA,

Geophysical Institute, Faculty of Science, The University of Tokyo.

(Read July 19, 1966.—Received Sept. 29, 1966.)

Abstract

The focal mechanism of the Hindu Kush earthquake of January 28, 1964 (focal depth; 207 km, magnitude; 6.1, after USCGS) is discussed by using body waves. On the basis of the experimental as well as theoretical result on the phase shift of the reflected waves in the case of two-dimensional model simulating the earth by Shimamura and Sato (1965), attention is given to the use of the reflected phases for the focal mechanism study in this paper.

The most probable solutions of the mechanism are numerically determined by using both the real polarization angles (ε) and the apparent polarization angles (γ), respectively, where the angle (γ) is obtained from the horizontal surface motion. The difference of the two solutions is found to be much less than the standard deviation of the solution. It is concluded that the earthquake can be explained by the double couple hypothesis since the observations of P and pP waves are sufficiently satisfied by the most probable solution determined from the S wave data alone by assuming the hypothesis.

It is suggested that the use of the pP wave is serviceable to the focal mechanism determination except in the case of shallow earthquakes, while the use of the PP wave is undesirable because of its $(-\pi/2)$-phase shift.

---

* Communicated by S. Omote.

** On leave from Geophysical Institute of Tehran University, Iran, to IISEE, Tokyo, Japan, as a UNESCO participant.

1. Introduction

In various fields of observational seismology it may be very important to determine accurately the focal mechanism of the earthquake concerned. Recently a few attempts were made to determine the focal mechanisms of intermediate and deep focus earthquakes by the analysis of surface waves and free oscillations of the earth excited by the earthquakes (Chander and Brune; 1965, Alsop and Brune; 1965). At present, it does not seem, however, that the focal mechanisms of the intermediate and deep focus earthquakes can be obtained accurately and uniquely by the use of such long-period surface waves.

The observations of the first motion of P waves may provide sufficient information for determining the fault plane solution in some cases of the earthquakes. In many cases, however, both of two P-nodal planes cannot be accurately determined from the P wave data alone because of the lack of data or the biased distribution of the observing points on the focal sphere. Assuming the double couple hypothesis, the method of least squares presented by Hirasawa (1966) may determine a statistically reliable solution by use of S wave data. Nevertheless an effort to increase the number of P wave data is desirable simultaneously with the use of the S wave data, since the double couple hypothesis assumed in the above numerical method should be justified for each earthquake in comparison with the P wave observations though the hypothesis has been commonly accepted for most of the earthquakes.

In this paper attention will be given to the use of pP-phase for the focal mechanism study on the basis of the experimental as well as theoretical result by Shimamura and Sato (1965).

According to the U.S. Coast and Geodetic Survey, the hypocentral coordinates of the Hindu Kush earthquake of January 28, 1964, studied in the present paper are as follows:

Origin Time; $14^{h}09^{m}17^{s}$ (GMT), Focal depth; 207 km,

Latitude; 36°30′N, Longitude; 70°54′E,

the magnitude being reported to be 6.1. Long period seismograms were provided by the USCGS. From seismogram readings of pP and sP-phases, observed arrival time differences between the pP and P and between the sP and P waves are shown in Fig. 1 in comparison with the theoretical curves obtained from the results by Jeffreys and Shimshoni (1964). In the figure the solid circles indicate the observations of $(sP-P)$ and the open circles those of $(pP-P)$, the numerals inside the parentheses being the focal depths (h) for the theoretical curves. It is concluded from the

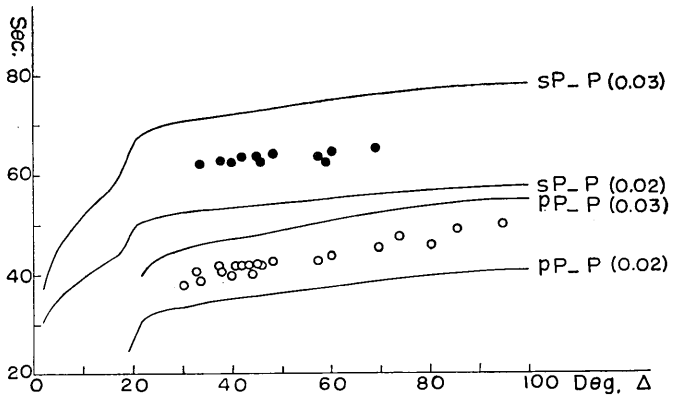

Fig. 1. Time intervals between pP and P waves and between sP and P waves versus epicentral distance.

The solid circle indicates the observed interval of (sP-P) and the open circle that of (pP-P). The numeral inside the parentheses is the focal depth corresponding to the theoretical curve by Jeffreys and Shimshoni (1964).

figure that $0.025R$ ($\approx$192 km) can be used in the present study as the focal depth instead of that given by USCGS.

2. P and pP Waves

The data of compression-rarefaction of the P wave are listed in Table 1. By using the equal area projection of the lower half of the focal sphere, Fig. 2 shows the radiation pattern of the observed P wave which is indicated by the circle without cross. The dashed curves in the figure show P-nodal planes of the graphical solution obtained from P wave data only by Takano (presented at the annual meeting of the Seismological Society of Japan, 1964). Although the graphical solution satisfies all of the P wave data except a few observations near the nodal lines, it may be apparent from the figure that it cannot be a unique solution because of the lack of adequate data.

Shimamura and Sato (1965) carried out an experiment on the phase shift of the reflected waves by using a disk as a two-dimensional model of the earth. According to their experimental as well as theoretical results, pP-phase suffers the phase shift by π radian due to the reflection at the surface in general (strictly speaking, π or 0 depending on the angle of incidence at the surface), while PP-phase should undergo the $(-\pi/2)$- or $(\pi/2)$-phase shift throughout its passage from the focus to an observing

Table 1. Seismogram readings for the P wave.

Station	Δ in degree	α_E in degree	Initial motion	i_d in degree
AAE	40.0	234.9	+	38.7
ADE	95.0	130.2	**	—
ANP	44.5	90.0	−	37.3
AQU	44.1	296.0	+	37.5
ATU	37.3	286.9	+	39.5
BAG	48.2	100.9	−	35.9
BUL	69.1	222.6	+	27.9
CHG	30.3	118.0	−	42.2
COP	43.4	315.3	+	37.7
HKC	39.9	98.5	−	38.7
HLW	33.6	270.3	+	40.8
HNR	94.8	98.1	+	20.4
IST	32.8	291.0	+	41.1
GUA	69.3	88.2	*,**	—
KEV	40.8	338.3	+	38.5
KON	45.0	321.0	+	37.0
KTG	57.0	336.3	+	32.4
MAL	58.9	294.8	+	31.6
MAN	49.6	102.5	*	—
MUN	80.2	142.2	+	23.8
NAI	49.2	227.8	+	35.5
NDI	09.4	143.9	−	81.9
NHA	42.0	115.2	−	38.1
NUR	37.8	324.3	+	39.4
PMG	84.7	105.7	−	22.4
PDA	73.3	304.7	+	26.4
PRE	73.8	219.5	+	26.3
PTO	60.1	301.0	+	31.2
QUE	07.1	208.8	−	90.2
RAB	85.5	98.5	+	22.2
SHI	16.9	250.9	+	62.1
SHL	21.0	115.4	−	50.0
STU	45.8	305.7	+	36.6
TOL	57.4	298.1	+	32.2
VIN	57.2	313.3	+	32.3
WIN	77.6	229.8	+	24.8

Δ: Epicentral distance.

α_E: Azimuth of the great circle path with respect to the epicenter.

i_d: Angle of incidence of the ray at the focus.

The positive sign of the initial motion means the vertical upward motion (Compression) and the negative sign the downward (Dilatation). The symbols *, ** represent the data for S and pP waves.

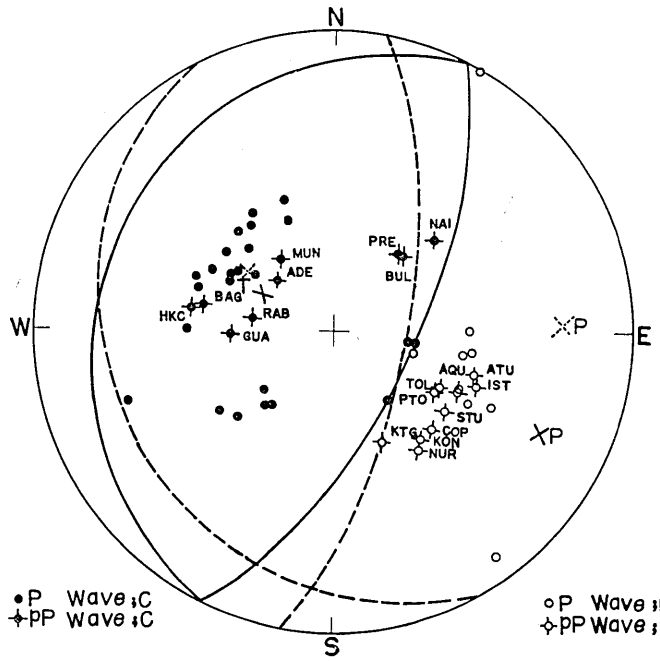

Fig. 2. The observations of P and pP waves and graphical solutions.

The dashed curves are P-nodal planes (solution 1) determined visually by Takano (1964), and the solid curves correspond to solution 2 obtained from P and pP observations.

point, which means that the wave form of the PP-phase should be different from that of direct P-phase. This fact had been suggested by Jeffreys and Lapwood (1957) in the case of a liquid sphere and seen in the theoretical seismograms computed numerically by Alterman and Abramovici (1965) in the case of a solid sphere, and was clearly ascertained from the experiment.

In order to increase the number of observations the use of the pP-phase may be suitable, since, if the wave form of the direct P wave is expected to be an impulse, the wave form of the pP-phase should be the same impulse in the opposite sense. On the other hand the use of the PP-phase may be undesirable, because a sharp onset of the phase cannot be expected in general. Figure 3 shows the seismograms of the vertical components on which the pP-phase are read without ambiguity, where the three-letter codes by **USCGS** are used to designate the stations. The epicentral distances and the magnifications of the seismographs are shown

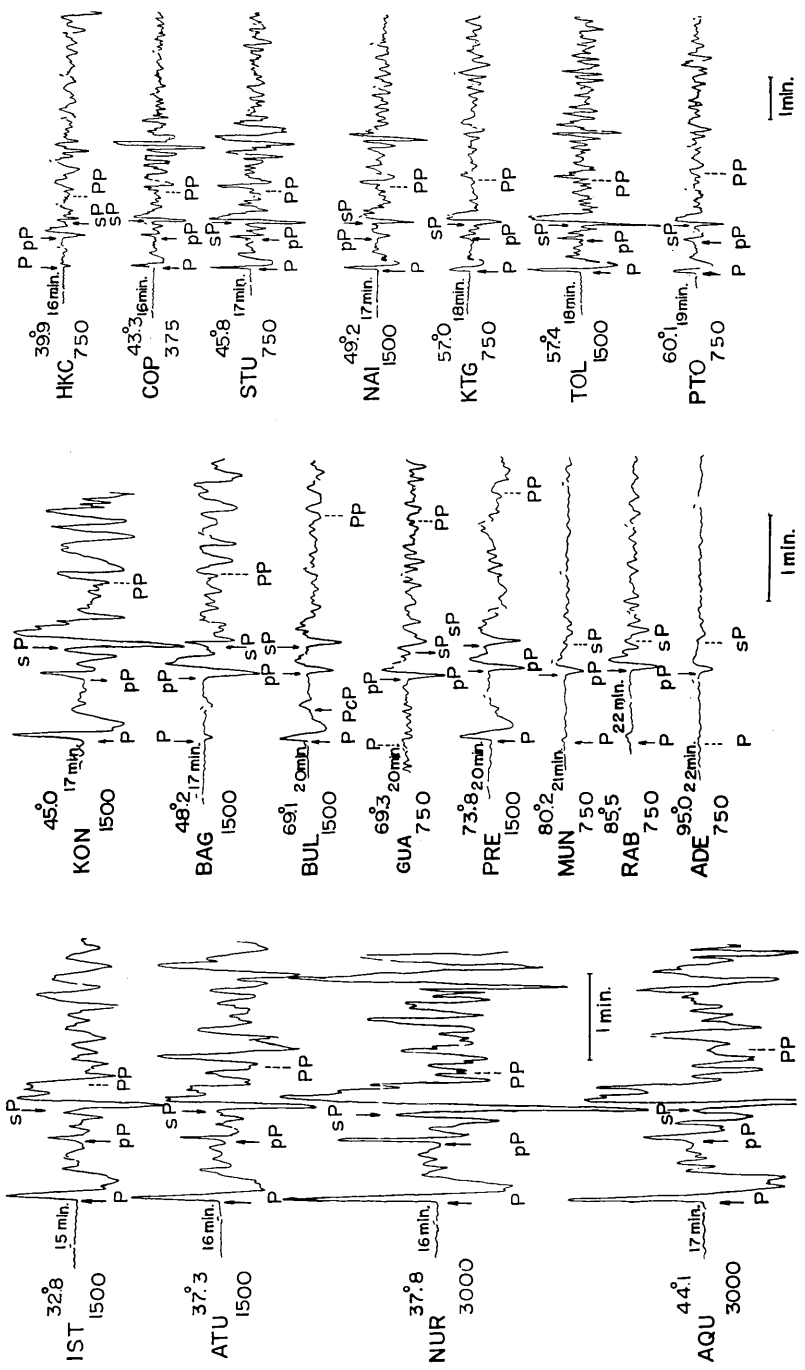

Fig. 3. Traced seismograms of the vertical components (30 sec–100 sec).
The epicentral distance and the magnification of the seismograph are shown.

Table 2. Seismogram readings for the pP wave.

Station	Initial motion*	i_d in degree
ADE	−	20.5
AQU	+	38.3
ATU	+	40.5
BAG	−	37.0
BUL	−	28.6
COP	+	38.5
HKC	−	39.7
IST	+	42.3
GUA	−	28.5
KON	+	38.0
KTG	+	33.4
MUN	−	24.3
NAI	−	36.5
NUR	+	40.4
PRE	−	26.8
PTO	+	32.1
RAB	−	22.6
STU	+	37.7
TOL	+	33.2

* Following the usual convention, the positive sign means **dC** and the negative sign **cD**. The angle of incidence (i_d) is measured from vertical upward.

in the figure. In the cases of the **GUA** and **ADE** observed amplitudes of the P wave are too small to determine the initial motion direction, and seismogram readings were not made for the P wave at the stations. In the figure the phase arrival time indicated by the dotted line is that expected for the Jeffreys-Bullen's travel time table. As may be seen in the figure, PP-phases have blunt onsets in all cases and the onsets of the major amplitude do not seem to coincide with the arrival times calculated from the Jeffreys-Bullen's table, while pP-phases have clear and sharp onsets, as is expected from the theory and the model experiment stated before.

Readings of the first motion of the pP-phase on the seismograms are tabulated in Table 2. After changing the sign of the motion direction due to the π-phase shift, the observations of the pP-phase are plotted in Fig. 2 where they are indicated by the circles with cross, the three-

letter codes also being added to them. It is found in the figure that the observation of pP-phase at **NAI** is inconsistent with the graphical solution shown by the dashed curves. From the seismogram recorded at **NAI** (cf. Fig. 3) the compression of the pP-phase is certainly correct, since there is no possible phase around the pP-phase (PcP-phase should appear between sP- and PP-phases).

The solution indicated by the solid curves in Fig. 2 is obtained visually so that all the data of the P- and pP-phases may be consistent with the solution. However, since any observation should have more or less the possibility that the reading of its sign is incorrect, resulting from high background noise, from misidentification of the phase, from reversed galvanometer wires in the worst case, etc., from the statistical point of view it is not so significant that the graphical solution does not have any inconsistent observation. In other words, it cannot be assured that the solution is the most probable one. Therefore, the graphical solution obtained here may be nothing but proof of the freedom of the graphical determination.

Both of the two graphical solutions are listed in Table 4 which will be given later.

3. Least Squares Solutions from S Wave Data

In this section the use of the polarization angle of the S wave is made to derive a fault plane solution independent of the P wave observations and to distinguish the source mechanism of the present earthquake.

Hirasawa (1966) has presented a numerical method of the least squares for the focal mechanism determination by use of S wave data. The substantial idea of the method is based upon the assumption that a finite set of the residuals of the polarization angles of the S waves for a particular earthquake is sampled from a population of the normal distribution, where the residual is defined by deviation of the observed polarization angle from that theoretically expected for the double couple model. By means of a statistical test he concluded that the above assumption is appropriate for practical purposes. In the present paper, therefore, this method is applied to obtain the most probable solution from the S wave data.

The polarization angle, ε, of the S wave is defined by the angle between the S movement and the vertical plane containing the seismic ray, that is,

$$\tan \varepsilon = (SH)/(SV) ,$$

where (SH) and (SV) are the amplitudes of **SH** and **SV** components of the S wave, respectively. An apparent polarization angle, γ, is defined by the relation,

$$\tan \gamma = \bar{u}_H/\bar{u}_R ,$$

where $\bar{u}_H$ and $\bar{u}_R$ are the horizontal components of the surface motion produced by the incidence of **SH** and **SV** waves, respectively. Assuming a homogeneous half space, the relation between γ and ε is expressed by the following formulae (Nuttli and Whitmore, 1962);

$$\tan \gamma = f_{(i_0, b_0/a_0)} \cdot \tan \varepsilon ,$$

$$f_{(i_0, b_0/a_0)} = \frac{\cos^2 2i_0 + 2 \sin i_0 \sin 2i_0 \sqrt{(b_0/a_0)^2 - \sin^2 i_0}}{\cos i_0 \cos 2i_0} ,$$

where, i_0 is the angle of incidence of the ray at the free surface, a_0 and b_0 are the velocities of P and S waves, respectively, and the incident angle is assumed to be less than the critical angle. The apparent polari-

Table 3. Polarization angles of the S wave.

Station	α_S in degree	i_d in degree	γ in degree	ε in degree
AAE	221.9	39.1	−66.1	−62.8
BAG	124.5	36.5	09.2	08.0
COP	271.0	38.0	38.6	34.6
GUA	124.1	29.8	34.1	31.3
KON	272.7	37.5	35.7	31.8
KTG	253.5	33.8	44.1	40.4
MAN	125.6	36.1	11.1	09.7
MUN	144.5	26.2	−02.5	−02.3
NAI	216.7	36.2	−78.9	−77.3
NHA	131.8	38.3	10.2	8.8
PMG	128.2	24.5	06.4	05.9
RAB	127.0	24.2	09.7	09.0
STU	261.6	37.2	15.3	13.3
VLN	251.3	33.8	26.3	23.4

α_S: Azimuth of the great circle path with respect to the station.
γ: Apparent polarization angle.
ε: Real polarization angle.

zation angles, γ, were determined by seismogram readings for 14 stations as shown in Table 3, where the sense of the S motion is disregarded and the sign convention given by Stauder (1962) is followed.

First, these observed angles (γ) are used to find the best solution as usual. In Figure 4, the dashed curves indicate the P-nodal planes of the least squares solution (1) obtained by the numerical method. The standard deviation of the polarization angles (γ) is estimated at 11°.0, no secondary minimum being found. In the figure P wave observations and the graphical solution (the solid curves) obtained from P and pP wave data are the same as in Fig. 2. It is found from the figure that the observations of P and pP waves are sufficiently satisfied by this least squares solution.

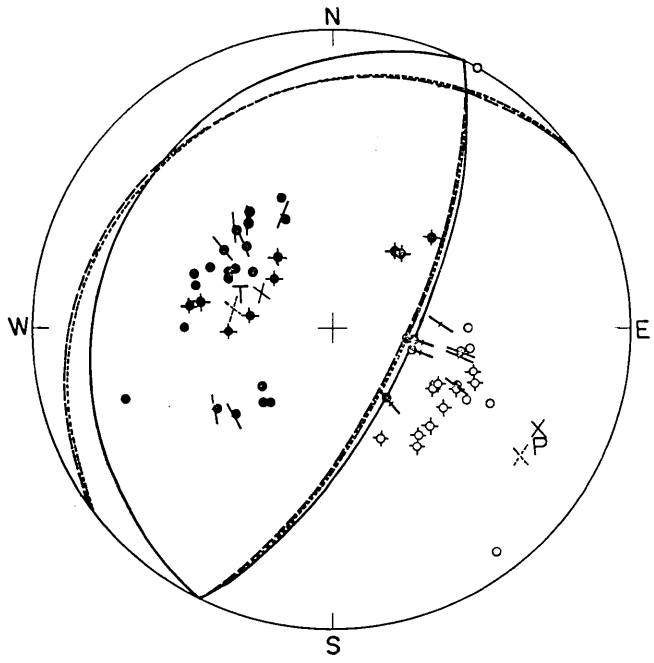

Fig. 4. The observations of the S wave and least squares solutions.

Illustrations of the observations of the P waves and the graphical solution 2 (solid curves) are the same as in Fig. 2. The dashed curves correspond to the least squares solution (1) derived from the apparent polarization angle (γ), and the dotted curves to the least squares solution (2) from ε. The pressure and tension axes illustrated by the crosses of dotted lines are those for solution (1).

Second, in order to see the difference between two solutions obtained from the apparent polarization angles (γ) and from the real polarization angles (ε), the values of ε are computed by making use of the table of $f_{(i_0, b_0/a_0)}$ which has been given by Nuttli and Whitmore (1962), where the Poisson's relation is assumed to hold. Providing that the shear velocity at the surface, b_0, can be taken to be 3.5 km/sec, the angle of incidence (i_0) at the surface is calculated by the formula;

Table 4. Fault plane solutions.*

		L.S. Sol. (1) (γ)	L.S. Sol. (2) (ε)	Graphical Sol. (1)	Graphical Sol. (2)
Source Parameters	(x_1')	−0.31840	−0.31821		
	(x_2')	0.22467	0.24448		
	(x_3')	−0.38076	−0.39841		
Elements of the Variance Matrix	(V_{11})	0.37312	0.39251		
	(V_{22})	0.03525	0.03393		
	(V_{33})	0.05073	0.05809		
	(V_{12})	0.06382	0.06115		
	(V_{13})	0.10866	0.12139		
	(V_{23})	0.00608	0.00550		
Variance in rad^2	$(\hat{\sigma}^2)$	0.03658	0.03532		
Standard Deviation	$(\hat{\sigma})$	11°.0	10°.8		
Nodal Plane (a)	Dip Direc.	− 35°.2±12°.8	− 37°.5±12°.8	−118°	− 64°
	Dip Angle	21.3 4.3	21.9 4.2	25	22
Nodal Plane (b)	Dip Direc.	116.1 3.8	115.8 3.7	100	116
	Dip Angle	71.1 2.0	70.3 2.1	70	68
Pressure Axis	Trend	124.0 5.2	123.3 5.2	88.5	116
	Plunge	25.5 2.6	24.7 2.7	23.5	23
Tension Axis	Trend	− 79.4 11.1	− 79.5 11.3	− 56.5	− 64
	Plunge	62.6 1.3	63.5 1.3	62	67
Null Axis	Trend	29.4 8.0	29.1 7.7	−175	26
	Plunge	9.5 8.2	9.0 8.1	14	0
Slip Angle	Plane (a)	63.0 12.1	65.0 11.9	54.5	90
	Plane (b)	80.0 4.1	80.4 4.0	75	90

* The notations should be referred to the paper by Hirasawa (1966). Graphical solution (1) has been given by Takano (1964) by using the P wave data only, and graphical solution (2) is determined visually from the P and pP wave data.

$$\sin i_0 = \frac{R-H}{R} \cdot \frac{b_0}{b_d} \sin i_d ,$$

where, R being the radius of the earth, H the focal depth (192 km), and b_d the shear velocity at the focus (4.6 km/sec after Bullen, p. 223; 1963). The values of ε are tabulated in Table 3.

The least squares solution (2) obtained from the ε is illustrated by the dotted curves in Fig. 4. The deviation of the solution (2) from the solution (1) is quite small, which may be natural since the use of observing points is confined to the stations for which the angles i_d are less than 40° as usual. The standard deviation of the polarization angles (ε) is estimated to be 10°.8. This value is a little smaller than that for the solution (1). It may be apparent without any statistical test, however, that the difference between the two standard deviations is not significant. The most probable values and their standard deviations for both of the two least squares solutions are listed in Table 4.

4. Discussions and Conclusions

Chander and Brune (1962) discussed the source mechanism of the Hindu Kush earthquake of July 6, 1962 (magnitude $6\frac{3}{4}$—7) by use of surface waves and body waves. According to their least squares revision the hypocentral coordinates of this earthquake are 36.48°N and 70.38°E, and the focal depth is 218 km±10 km. This hypocenter is very close to that of the earthquake discussed in the present study, and the difference may be less than about 60 km. They have presented a few examples of the P and S pulses recorded by the long-period seismographs in their paper. These wave forms are quite similar to those of the P pulses given in Fig. 3. It follows that the P pulse from the present earthquake of 1964 is regarded as an impulse for the long-period standard seismograph.

However, the fault plane solution (the nodal planes; strike EW and dip 78°±6°S, strike EW and dip 12°±6°N) adopted by Chander and Brune for the earthquake of 1962 is not quite like that of the present earthquake. The trend and plunge of the pressure axis are 180° and 33° for the 1962 shock, and 124°.0±5°.2 and 25°.5±2°.6 for the other. This difference may be a more than permissible variation in the solutions.

Ritsema (1955) investigated the mechanism of many Hindu Kush earthquakes that occurred between 1917 and 1952, where the first motion data of P waves from all the earthquakes were superposed to give a single solution as if the P waves were those from only one shock. He

found that the P-axis lies almost horizontal in the direction SE—NW and that this axis is not in contradiction with the almost NE—SW trending Hindu Kush mountain system.

Recently, Ritsema (1966) presented fault plane solutions of many intermediate and shallow earthquakes that had occurred in the Hindu Kush region, and obtained a kind of average fault plane solution for each of the intermediate (150–250 km) and shallow (0–100 km) earthquakes. He derived the interesting conclusion that the direction of the maximum stress component of the average solution for the shallow shocks is almost perpendicular to the structural trend of the Hindu Kush mountain system and, on the other hand, that for the intermediate shocks is approximately perpendicular to the Himalayas and Karakorum mountain ranges. He also determined a fault plane solution from the P wave data for the earthquake discussed in the present study, that is, the P-nodal planes; strike N50°E and dip 62°SE, strike N50°E and dip 28°NW. The difference between his solution and the least squares solution obtained here may be in the order of the error, while the least squares solution as well as his solution is significantly different from the average solution for the intermediate shocks and is rather close to that for the shallow shocks. It is a very interesting question whether this difference of the solutions is merely due to various preferred orientations of the slip plane at different hypocenters, in spite of the existence of a broad and constant system of the tectonic force, or really due to different local stress systems.

Hodgson and Adams (1958) have examined the consistency of the data obtained from the reflected phases with the fault plane solution and found that the percentages of inconsistencies of pP and PP wave data are both nearly 50%. They suggested that the data which have been reported by many different observers should not be used for the focal mechanism determination. However, the above high percentage of inconsistancies of the PP wave may be attributed to its $(\pi/2)$-phase shift, and difficulty of finding the first motion of the PP wave may be understood from the seismograms in Fig. 3. Regarding the pP wave, it seems that the use of the pP phase in the case of shallow earthquakes may be the reason for the high probability of inconsistent observation. In the cases of intermediate and deep earthquakes it is apparent from the seismograms presented in this paper that the first motion of the pP-phase can be read without question. The fact that the first motion data from pP waves are completely consistent with the least squares solution is very important, since the solution has been obtained independently of the

observations of P and pP waves.

In comparison with the conclusion by Hodgson and Adams (1958), there are some examples in which the pP wave is successfully used for the focal mechanism study, for instance, the study by Ritsema (1955) mentioned above, and that by Honda (1962, p. 42). However, at a time when knowledge about the phase shift of the reflected waves has been brought to light by theoretical as well as experimental studies, it may be meaningful to make it clear that the use of pP waves is serviceable to the focal mechanism determination except in the case of shallow earthquakes and that, on the contrary, the use of PP wave type is undesirable in general, where the PP wave type means the wave for which the phase shift is $\pm\pi/2$, for example, PP, pPP, etc.

In deriving the polarization angle of S wave, an effect of the crustal layering should be taken into account. However, consideration on this effect is not given in the present paper and will be left as a future problem for the following reasons:

1. The local crustal structure assigned to each station is unknown.
2. In the case where the incident S wave can be regarded as an impulse, it may be doubtful to apply directly such a result of the effect for the periodic case as given by Nuttli (1964).

Main results are summarized as follows:

1. A fault plane solution of the Hindu Kush earthquake of Jan. 28, 1964 is obtained by using the data of apparent polarization angles (γ) of the S wave, that is, the P-nodal planes are (dip direction $= -35.^{\circ}2 \pm 12.^{\circ}8$, dip angle $= 21.^{\circ}3 \pm 4.^{\circ}3$) and ($116.^{\circ}1 \pm 3.^{\circ}8$, $71.^{\circ}1 \pm 2.^{\circ}0$), and the pressure axis is (trend $= 124.^{\circ}0 \pm 5.^{\circ}2$, plunge $= 25.^{\circ}5 \pm 2.^{\circ}6$).

2. A fault plane solution of the same earthquake is obtained from the real polarization angles (ε) which are determined by the ratios of the amplitudes of incident **SH** to those of **SV** waves. The difference of this solution from the former obtained by (γ) is very small and much less than the standard deviation of the solution. Although the estimated variance of the polarization angles (ε) is a little smaller than that for the angles (γ), the difference is insignificant. Therefore, the use of the apparent polarization angle (γ) may be appropriate for the focal mechanism determination, if they are obtained from the stations at which the incident angles at the surface are less than about 30°.

3. The most probable solution derived from the S wave data alone by assuming the double couple model is quite satisfactory to the observations of P and pP waves. It follows that the Hindu Kush earthquake

can be explained by the double couple hypothesis.

4. The pressure axis corresponding to the least squares solution for this earthquake is significantly different from that of the average solution derived by Ritsema (1966) from many Hindu Kush earthquakes with focal depths 150–250 km, and is rather similar to that of the average solution for shallow earthquakes (0–100 km) in the same region directed almost perpendicularly to the structural trend of the Hindu Kush mountain system.

5. The pP wave data may be useful for the focal mechanism determination, since the first motion can be distinguished without ambiguity and the agreement of the observations of the pP waves with the solution from the S wave data is satisfactory. Moreover, it may be better to avoid the use of PP waves for this purpose, since the PP wave would suffer $(-\pi/2)$-phase shift, or the wave form of the PP would be different from that of the direct P wave.

Acknowledgements

The authors wish to thank Dr. R. Sato, Dr. K. Takano, and Mr. H. Shimamura for their helpful discussions. The authors are indebted to Dr. S. Omote, acting director of the IISEE, and Prof. T. Asada for their kind guidance in the course of this study.

References

ALSOP, L. E. and J. N. BRUNE, 1965. "Observation of Free Oscillations Excited by a Deep Earthquake", *Journ. Geophys. Res.*, **70**, 6165-6174.

ALTERMAN, Z. and F. ABRAMOVICI, 1965. "Propagation of a *P*-Pulse in a Solid Sphere", *Bull. Seism. Soc. Amer.*, **55**, 821-861.

BULLEN, K. E., 1963. "*An Introduction to the Theory of Seismology*", Cambridge, University Press, 3rd ed.

CHANDER, R. and J. N. BRUNE, 1965. "Radiation Pattern of Mantle Rayleigh Waves and the Source Mechanism of the Hindu Kush Earthquake of July 6, 1962", *Bull. Seism. Soc. Amer.*, **55**, 805-819.

HIRASAWA, T., 1966. "A Least Squares Method for the Focal Mechanism Determination from *S* Wave Data; Part I, Part II", *Bull. Earthq. Res. Inst.*, **44**, 901-918, 919-938.

HODGSON, J. H. and W. M. ADAMS, 1958. "A Study of the Inconsistent Observations in the Fault-Plane Project", *Bull. Seism. Soc. Amer.*, **48**, 17-31.

HONDA, H., 1962. "Earthquake Mechanism and Seismic Waves", *Geophysical Notes*, Tokyo Univ., **15**, *Supplement*, 1-97.

JEFFREYS, H. and E. R. LAPWOOD, 1957. "The Reflexion of a Pulse within a Sphere", *Proc. Roy. Soc. London A*, **241**, 455-479.

JEFFRFYS, H. and M. SHIMSHONI, 1964. "The Times of *pP*, *sS*, *sP* and *pS*", *Geophys. Journ.*, **8**, 324-337.

NUTTLI, O. and J. D. WHITMORE, 1962. "On the Determination of the Polarization Angle of the *S* Wave", *Bull. Seism. Soc. Amer.*, **52**, 95-107.
NUTTLI, O., 1964. "The Determination of *S*-Wave Polarization Angles for an Earth Model with Crustal Layering", *Bull. Seism. Soc. Amer.*, **54**, 1429-1440.
RITSEMA, A. R., 1955. "The Faultplane Technique and the Mechanism in the Focus of the Hindu Kush Earthquakes", *Indian Journ. Meteor. Geophys.*, **6**, 41-50.
RITSEMA, A. R., 1966. "The Fault-Plane Solutions of Earthquakes of the Hindu Kush Centre", *Tectonophysics*, **3**, 147-163.
SHIMAMURA, H. and R. SATO, 1965. "Model Experiments on Body Waves—Travel Times, Amplitudes, Wave Forms and Attenuation", *Journ. Phys. Earth*, **13**, 10-33.
STAUDER, W., S. J., 1962. "The Focal Mechanism of Earthquakes", *Advances in Geophysics*, **9**, 1-76.

67. *S* 波による Hindu Kush 地震 (1964年1月28日) のメカニズム—*pP* 波の利用について

建築研究所 国際地震工学部 A. HEDAYATI
東京大学理学部 地球物理学教室 平沢朋郎

1964年1月28日に起つた Hindu Kush 地震 (深さ 207 km, マグニチュード 6.1) のメカニズムを実体波の観測により調べた. 主な結果は次の通りである.

1. 水平二成分の振幅比から求められた *S* 波の polarization angle を使つて, double couple を仮定した最小二乗法により fault plane solution が得られた. 二つの *P* 波節面は, dip direction = N35°.2±12°.8W; dip angle = 21°.3±4°.3, および, dip direction = N116°.1±3°.8E; dip angle = 71°.1±2°.0 であり, また主圧力の軸は trend = N124°.0±5°.2E; plunge = 25°.5±2°.6 である.

2. 入射 SH および SV 波の振幅比で表わされる真の polarization angle を使つて得られた fault plane solution と上述のそれとの差は最小二乗解の標準偏差よりはるかに小さい.

3. *S* 波データから求められたメカニズムは *P* 波および *pP* 波の初動方向の観測を十分に満足する. したがつてこの地震は double couple のモデルで説明される.

4. 浅発地震の場合を除いて, 一般に *pP* 波の初動は非常に明瞭であり, また上述の通り *pP* 波の初動方向は独立に *S* 波より決められたメカニズムによつて十分説明されることから, *pP* 波の利用はデータの増加に役立つであろう. 一方, 島村—佐藤 (1965) の研究に明らかなように, *PP* 波の波形は *P* 波のそれと異なり, 初動方向の読みとりが困難である.

5. この地震の主圧力の方向は, Ritsema (1966) によつて与えられた Hindu Kush 地方の稍深発地震 (150-250 km) の平均的なメカニズムにおけるそれ (Himalayas-Karakorum mountain system にほぼ直交) と有意義に異なり, むしろ浅発地震 (0-100 km) の平均的な主圧力の方向 (Hindu Kush mountain system にほぼ直交) に近い.